91602
new 82-10

COMPLIMENTARY COPY
Please Credit Ontario Hydro Research if
Reproduced in Whole or in Part

ontario hydro
research division

Assessment of a Bruce NGS B Unit 6 Steam Generator Tube

Report No. 90-305-K

P.J. King, Corrosion Engineer, and A.M. Brennenstühl, Corrosion Engineer
Corrosion and Tritium Technology Section

and

G. Bellamy, Senior Engineer
Materials Technology Section

Metallurgical Research Department

Abstract

This report summarizes the information gathered from examinations of tube R57S32 from Bruce Unit 6 steam generator 6. A heavy, black magnetite deposit covered the tube above the rolled joint. Chronic oxygen inleakage is a major contributor to the formation of such deposits. Small nodular deposits were scattered over the surface. These contained impurities normally associated with untreated lake water. Shallow non-uniform corrosion and pitting, to a maximum depth of 60 μm, was found beneath the magnetite and nodular deposits. Attack was caused by aggressive solutions containing lakewater impurities, particularly chlorine. Examination of a tube from the same boiler, but removed in the spring of 1989, revealed no such corrosion, indicating that the water treatment plant acid excursion of July 1989 contributed to the corrosion. Steam generators of the other 3 units of Bruce B station are likely to have suffered similar attack.

job	file	date	report no.
7406-82-042	827.21	January 29, 1991	90-305-K

91-07177/

LEGAL NOTICE

This report was prepared by Ontario Hydro and, while effort has been made to assure the accuracy and applicability of the material contained herein, neither Ontario Hydro nor any person acting on its behalf:

(a) makes any warranty, express or implied with respect to the use of any information, apparatus, method or process disclosed in this report or that such use may not infringe privately owned rights; or

(b) assumes any liabilities with respect to the use of, or for damages resulting from the use of, any information, apparatus, method or process disclosed in this report.

91602
r new 82#10

ontario hydro
research division

Executive Summary

Assessment of a Bruce NGS B Unit 6 Steam Generator Tube

P.J. King, A.M. Brennenstühl, and G. Bellamy
Metallurgical Research Department

This report summarizes the information gathered from examinations of tube R57S32 from Bruce Unit 6 steam generator 6. Standard metallographic procedures were followed for the preparation and examination of tube samples. Tubes and deposits were examined by optical and scanning electron microscopy (SEM), and deposit analyses were obtained by energy dispersive x-ray spectroscopy, X–ray photoelectron spectroscopy , and Auger electron spectroscopy .

Deposits

Visual and microscopic examination of the tube revealed a heavy, black magnetite deposit above the rolled joint. Below the rolled joint,the tube was dulled by a thin surface film. Small nodular deposits were randomly scattered over the surface both above and below the rolled joint. SEM examination of the nodules revealed micro-cracked material, quite different from the surrounding regions.

Detailed examination showed that the deposit layer had a multi-layer structure and ranged in thickness from only a few micrometres to 10 μm to 20 μm. The deposit was compact and dense, with a generally smooth topography. Analyses showed that the general deposit contains mainly iron, that the nodules are high in chromium and chlorine, and that some sulphur is present. Other elements variously found included calcium, silicon, and titanium, among others.

Corrosion

The metallurgical examinations indicated that the tubing is in generally good condition. Although of marginally low hardness and somewhat high sulphur content, this has little implication regarding mechanical integrity and corrosion performance. The dual-etch procedure revealed a nearly complete inter-granular carbide network, with relatively little intra-granular carbide. This condition is believed to be resistant to stress corrosion cracking.

Outside surface examination after chemical de-scaling revealed scattered areas of shallow non-uniform corrosion, < 5 μm deep. Pitting, 20 μm to 60 μm deep, occurred within many of the non-uniform corrosion sites. Morphological features of the attack include facetting, crystallographic striations, and grain boundary outlining (very shallow intergranular attack). Tube attack was located throughout the length of tube above the tubesheet; however, the occurrence and severity of the non-uniform corrosion was slightly greater near the rolled joint than further up the tube. Shallow and sparsely distributed non-uniform corrosion associated with nodular deposits was also observed on the section of tube between the rolled joints. There was no pitting associated with these sites.

job	file	date	report no.
7406-82-042	827.21	January 29, 1991	90-305-K

The observed attack is superficial and slight in extent, but widespread in distribution. The non-uniform corrosion penetrates about 1% of tube wall thickness and the maximum pit depth of 60 μm is only 5% of tube wall thickness. The surface dimensions and population suggest that about 1% of the examined tube surface is affected. The extent of corrosion throughout the entire steam generator cannot be determined from only one tube; however, it must be concluded that similar corrosion is present on other tubes.

Mechanisms

The general magnetite scale on the tubes is produced by the deposition of carbon steel corrosion products. The bulk of these corrosion products are produced in the feedtrain and transported into the steam generators as suspended particulate or dissolved species. A major contributor to the production of corrosion products is oxygen introduced by air in-leakage.

A possible mechanism of corrosion is proposed as follows.

- General tube surface deposits promote the formation of concentrated chemical environments consisting of lake water impurities (particularly chloride ions) close to tube surfaces. Acid sulphate, introduced during the water treatment plant upset, would also contribute to the concentrated environments.

- Corrosion proceeds under the influence of the anionic contaminants. Corrosion products accumulate in the vicinity of active sites, forming nodules and irregularities within the general deposit.

Integrity

Steam generator integrity is not immediately compromised by the degree of attack observed. No more than a 1% strength loss would be expected as a result of the observed corrosion. This should be well accommodated by design margins and safety factors. Because of the continued presence of tube deposits, aggressive crevice conditions could reform during normal operation or upsets. Continued degradation would pose a threat to tube integrity in the long term.

Implications and recommendations

The principal implications for operation are that good water chemistry and minimum air in-leakage must be rigourously maintained to avoid corrosion damage. It should be remembered that normal make-up [or even small condenser leaks] can supply sufficient contaminant to generate aggressive conditions. Remedial action should be taken immediately in the event of a chemical excursion.

Better information is necessary about the extent of corrosion. For this, a larger sample size is required to represent, adequately, the population of tubes in the bundle and to assign statistical significance to the results. It is recommended that additional tubes be obtained for this purpose at every reasonable opportunity. This would provide additional information for reference in future condition-monitoring and assessments of steam generator tubes.

Table of Contents

		Page
1	Introduction	1
2	General description of the tube sample	1
3	Analytical techniques	1
3.1	Metallographic methods	1
3.2	Elemental analysis methods	2
4	Results	2
4.1	Tube material	2
4.2	Tube surfaces	3
4.3	Deposit characteristics	4
4.4	Deposit chemistry	4
5	Discussion	6
5.1	Metallurgical condition	6
5.2	Corrosion damage	7
	Extent	7
	Causative factors	7
5.3	Deposits	8
	Origins	8
5.4	Implications	9
	Integrity	9
	Other steam generators and reactor units	9
	Operation	9
6	Recommendations	10
7	Conclusions	10
Acknowledgements		11
APPENDIX 1		24
APPENDIX 2		28
APPENDIX 3		29

List of Tables

		Page
Table 1	Chemical analysis of tube material	3
Table 2	Estimates of extent of corrosion damage	3
Table 3	EDS Analyses	4
Table 4	Qualitative EDS, relative composition by peak height ratios	5
Table 5	XPS ratios	6
Table 6	AES Ratios	6
Table A1	Semi-quantitative EDS	29
Table A2	Qualitative EDS	30
Table A3	XPS summary	31
Table A4.	XPS composition from the bronze film on the tube surface below the rolled joint	31
Table A5	XPS composition from a nodule below the rolled joint	31
Table A6	XPS composition from the deposit above the tube sheet	31
Table A7	AES Spectra from the Irregularities (Atomic %)	32

List of Figures

		Page
Figure 1	Illustrations of the general surface features of tube R57S32.	12
Figure 2	The general microstructure of tube R57S32...	13
Figure 3	Cross-sections of the tube at the outside surface...	14
Figure 4	Micrographs of tube R57S32 after chemical descaling by APAC...	14
Figure 5	Micrographs of tube R57S32 after chemical descaling by APAC...	15
Figure 6	Scanning electron micrographs of a cross-section through the deposit layer...	16
Figure 7	Scanning electron micrographs of a cross-section through the deposit layer...	16
Figure 8	Outside surface condition of tube R57S32.	17
Figure 9	Another micrograph of the outside surface of tube R57S32...	18
Figure 10	A micrograph of the outside surface of tube R57S32...	18
Figure 11	A nodule above the rolled joint.	19
Figure 12	General features within a nodule after removal of the outer layer.	19
Figure 13	Details of features within a nodule after removal of the outer layer.	20
Figure 14	EDS maps for the nodule shown in Figure 13a.	21
Figure 15	A portion of the XPS spectrum for the general deposit above the rolled joint...	22
Figure 16	AES maps for the nodule shown in Figure 8b after 1 minute of sputtering.	23

91601
new 82-10

ontario hydro
research division

TO: Mr. R.W. Patterson
CPSD
A08 H6

Assessment of a Bruce NGS B Unit 6 Steam Generator Tube

P.J. King, A.M. Brennenstühl, and G. Bellamy

1 Introduction

This report summarizes the information gathered from examinations of tube R57S32, removed from Bruce Unit 6 steam generator 6 in November 1989. Preliminary results of the investigation were reported in March (P.J. King, memo to Dr. P.E. Doherty, 1990 March 16, File 827.21).

The object of the examination was to establish the condition of the tube with respect to corrosion and deposit build-up. Work was focused in three areas: tube surface assessment, deposit analysis and characterization, and tubing metallurgical condition.

2 General description of the tube sample

Visual and low power stereoscopic examination of the outside surface revealed a heavy, black magnetite deposit covering the tube above the rolled joint. Below the rolled joint,the tube had a metallic lustre, dulled by a thin surface film. Small nodular deposits and circular discolourations were randomly scattered over the surface both above and below the rolled joint. These features were more visible on the part of the tube below the rolled joint. No tube surface degradation was apparent on the tube in the as-received condition.

Figure 1 illustrates these general features.

3 Analytical techniques

Numerous analytical techniques were used to obtain detailed information on the tube and deposits. The following paragraphs provide information about these methods.

3.1 Metallographic methods

In general, standard metallographic procedures were followed for the preparation and examination of tube samples. Longitudinal and transverse metallographic sections were cut to reveal microstructural detail in pertinent areas both above and below the rolled joint. A two stage metallographic etching procedure was used to reveal, sequentially, the carbide distribution and the grain boundaries. The procedure, based on EPRI recommendations, is attached as Appendix 1.

Hardness measurements were obtained on the prepared metallographic sections, and tube wall thickness measurements were made using a calibrated microscope graticule on the transverse sections.

Because minor corrosion damage is often very difficult to detect on cross-sections, small coupons were removed for surface examination. After initial examination, regions of interest were chemically

descaled by an APAC procedure, Appendix 2, to facilitate corrosion assessment. Small segments of tubing were bent and cross-sectioned to improve the detectability of intergranular attack (IGA).

Visual examination and optical microscopy were used to reveal general details of surface condition and to identify features for detailed examination. The scanning electron microscope (SEM) provided good quality images and, with its enhanced depth of field, was used for the detailed examinations.

The depth of corrosion attack was estimated by re-focussing measurements on a light microscope; diameters were measured with a calibrated eyepiece graticule. The population distribution of localised corrosion was estimated by pit counts over a number of tube regions of approximately 1 cm^2. The corroded area on each tube region was estimated by taking the product of the number of sites and the average site area. An area coverage was calculated for each region as the ratio of the corroded area to the total area. Statistics of these measurements were computed for 20 regions.

3.2 Elemental analysis methods

An SEM capable of energy dispersive x-ray spectroscopy (EDS) was used to obtain general surveys of elemental composition, representing material to a depth of about 1 μm from the surface being examined. Semi-quantitative analysis, particularly suitable for assessing relative compositions, is readily obtained from SEM/EDS. A JEOL JSM35 scanning electron microscope fitted with a Link Systems energy dispersive analyser was used for most of the analyses reported here.

EDS data were obtained from areas of about 100 μm^2 on tube surfaces and about 1 μm^2 to 10 μm^2 on prepared cross-sections. These were supplemented by spot analyses and X-ray mapping of selected features.

X-ray photoelectron spectroscopy (XPS) was employed to probe the outer surface of selected surface features. This technique was chosen for its ability to probe the outer surface of the tube (information is obtained from a depth of only 30 Å) and to provide detailed chemical binding information.

XPS was carried out on an analysis area of approximately 600 μm x 600 μm using Al-Kα radiation; a Surface Science XPS - 100 was used throughout. Spectra were first obtained from the as received surface of the tube sample. The surface was then sputtered with a 4 KV argon ion beam to remove ambient contamination. Spectra were collected after various sputtering times. Deconvolution of specific spectra was performed in order to obtain chemical binding information.

Auger electron spectroscopy (AES) was also used to analyse selected surface features. The relevant advantage of this technique over XPS is the high lateral resolution(< 0.1 μm), allowing information to be obtained from very small areas. The spatial distribution of specific elements can be mapped with this technique.

AES was performed on the tubes subsequent to the XPS examination using a 5 KV electron beam. Again spectra were obtained from the as received surface and after sputtering. A 4 KV argon ion beam was employed to removed material from the outer surface.

4 Results

4.1 Tube material

The dual-etch procedure revealed a nearly complete inter-granular carbide network, with relatively little intra-granular carbide. Figure 2 shows the general microstructure, consisting of equiaxed grains with a grain size of about 30 μm.

Vickers' hardness tests on the prepared cross-sections returned uniform values of 134 H.V. in undeformed material above the rolled joint and 160 H.V. within cold worked material in the rolled joint.

A full chemical analysis of the tube material appears in Table 1.

Table 1. Chemical analysis of tube material
(ref: Chemical Research Department report number CE-90-0164-K)

Item	Elemental Analysis (wt%)										
	C	Mn	Si	S	Cr	Ni	Ti	Fe	Cu	Mo	Nb
Tube R57-S32	0.025	0.19	0.092	0.03	15.46	75.27	0.38	8.53	0.01	0.007	0.008
ASME SB 163, Alloy UNS N06600	0.15 max.	1.0 max.	0.5 max.	0.015 max.	14.0 - 17.0.	72.0 min.	-	6.0 - 10.0.	0.5 max.	-	-

Measurements of tube wall thickness gave results of 1.03 within the rolled joint and 1.06 mm just outside, for a wall reduction in the rolled joint of about 3%.

4.2 Tube surfaces

Cross-sections revealed no gross corrosion damage on either inside or outside surfaces; however, Figure 3 indicates the possibility of superficial intergranular attack (IGA) on the outside. Examination of tube surfaces after chemical descaling failed to confirm the presence of IGA. Similarly, cross-sections of bent samples did not show any general IGA.

Outside surface examination revealed scattered areas of shallow non-uniform corrosion, < 5 μm deep. Pitting, 20 μm to 60 μm deep, occurred within many of the non-uniform corrosion sites, see Figures 4 and 5. Morphological features of the attack include facetting, crystallographic striations, and grain boundary outlining (very shallow IGA). Table 2 summarizes the measured diameter, depth, and population of pitting. Tube attack was located throughout the length of tube above the tubesheet; however, the occurrence and severity of the non-uniform corrosion was slightly greater near the rolled joint than further up the tube.

Table 2. Estimates of extent of corrosion damage
(values given are average and [maximum])

Corrosion sites	Diameter (μm)	Depth (μm)	Density (sites/cm^2)	Area coverage (%)
Small, single	100 [200]	6 [10]	15 [56]	0.2 [1]
Large clustered	495 [800]	12 [30]	4 [20]	0.8 [4]
Pits	127 [250]	41 [60]	2 [7]	0.04 [0.4]
All	180 [800]	10 [60]	20 [56]	1 [4]

Sparsely distributed non-uniform corrosion was also observed on the section of tube between the rolled joints. This attack appeared to be associated with nodular deposits. It was shallower and less frequent than attack above the rolled joint; also, there was no pitting associated with these sites.

The inside surfaces were examined only on the metallographic cross-sections. As already noted, there was no indication of gross corrosion damage; nor was there any evidence of IGA, nor stress corrosion cracking (SCC) at the rolled joint. The entire inside surface of the tube was covered with a black, crystalline deposit layer. Examination of this deposit did not form part of this investigation.

4.3 Deposit characteristics

As already noted, the tube above the rolled joint was covered by a continuous, black, crystalline deposit layer with a scattering of circular discolourations and lighter-coloured nodular deposits. Although the deposit is slightly thicker near the rolled joint, there was no physical indication of the presence of a sludge pile.

The deposit layer is generally only a few micrometres in thickness; however, within a few millimetres of the roll transition the deposit is thicker, 10 µm to 20 µm, and has a multi-layer structure. The deposit appears compact and dense, with a generally smooth topography and uniform thickness. On a previously removed tube, the deposit appeared more porous, with a rough topography and non-uniform thickness. Figures 6 and 7 illustrate these features.

Figures 8a and b illustrate the outside surface condition in areas above and below the rolled joint. The thick magnetite deposit is clearly visible in figure 8a. The crystalline nature of the general deposit was revealed by SEM. Figure 9 shows that it is composed of small crystals approximately 2 µm in size. Figure 10 illustrates the deposit and an area of dark discolouration.

SEM examination of the nodules revealed micro-cracked material, quite different from the surrounding regions, shown in Figures 8a and 11. Figures 12 and 13 illustrate features within a nodule; under the surface is another layer of material, also often micro-cracked, and areas of metal covered by a thin oxide layer.

4.4 Deposit chemistry

A summary of the elemental analyses is presented here; Appendix 3 contains the full results.

Semi-quantitative EDS, Table 3, shows that the general deposit contains mainly iron, that the nodules are high in chromium and chlorine, and that some sulphur is also present.

Table 3. EDS Analyses
(see also Appendix 3, Table A1)

Location	Element (Wt.% conc)					
	Ni	Cr	Fe	Cl	S	Ti
Black deposit, above rolled joint	8	3	76	0	2	1
Nodular, micro-cracked deposit, below rolled joint	28	34	13	6	4	4

Other EDS spectra did not show sulphur but confirmed the presence of chlorine and high chromium in some locations. The summary data in table 4 show several features, as listed here.

- metal exposed by the removal of surface deposits is very similar to base metal
- nodules are enriched in chromium and contain chlorine
- the oxide film at the metal surface is depleted in nickel and enriched in iron
- the general deposit is high in iron; chromium is variable; and there is little chlorine

Other elements variously found by EDS include calcium, silicon, titanium, manganese, magnesium, aluminum, and potassium, as shown in the appendix.

Table 4. Qualitative EDS, relative composition by peak height ratios
(see also Appendix 3, Table A2)

Item	Ratios			
	$Ni_{/(Ni+Fe+Cr)}$	$Cr_{/(Ni+Fe+Cr)}$	$Fe_{/(Ni+Fe+Cr)}$	$Cl_{/(Ni+Fe+Cr)}$
Base metal	0.68	0.20	0.11	0.00
	0.60	0.24	0.17	0.00
Exposed metal	0.66	0.24	0.10	0.02
	0.58	0.25	0.16	0.00
	0.66	0.21	0.13	0.00
Nodule	0.57	0.34	0.09	0.16
	0.37	0.45	0.17	0.08
Oxide film	0.31	0.17	0.53	0.00
Deposit	0.04	0.01	0.94	0.00
	0.04	0.02	0.94	0.00
	0.10	0.02	0.88	0.00

X-ray maps for a nodule are shown in Figure 14; data for iron, chromium, nickel and chlorine are given.

XPS analysis of the tarnish film below the rolled joint prior to sputtering revealed the presence of oxygen, sodium, nitrogen, chlorine, sulphur, silicon, nickel and iron. Nodular deposits both above and below the rolled joint were similar in composition and were not much different from the tarnish film. XPS spectra from above the rolled joint but some distance from the nodules revealed the presence of copper, iron, oxygen, sodium, nitrogen, calcium, magnesium, carbon, chlorine, phosphorous and silicon. In particular, iron and chlorine concentrations were much higher than in the other regions, Table 5.

Table 5. XPS ratios
(see also Appendix 3, Tables A3 to A6)

Location	sputter time [sec]	$Ni_{/(Ni+Fe+Cr)}$	$Cr_{/(Ni+Fe+Cr)}$	$Fe_{/(Ni+Fe+Cr)}$	$Cl_{/(Ni+Fe+Cr)}$	$O_{/(Ni+Fe+Cr)}$
Tarnish, below rolled joint	300	0.21	0.07	0.71	0.03	1.12
Nodule, below rolled joint	300	0.16	0.03	0.81	0.02	1.09
Deposit, above rolled joint	60	0.08	0.03	0.88	0.17	4.07

Deconvolution of the carbon spectrum indicated the presence of carbide, hydrocarbon, alcohol groups, and carboxyl groups. The chlorine spectrum indicated inorganic and probably organic chloride. Examination of the nickel peaks suggested that nickel was present as nickel hydroxide and nickel metal, see Figure 15. The Ni(2p) spectrum shows a charge-shifted nickel metal peak and a $Ni(OH)_2$ sp peak. The binding energy for the iron indicates that it is magnetite.

AES spectra were also collected from a nodule. Figure 16 shows maps for selected elements. The spectra indicate that the nodules are comprised of Cl, C, N, Ca, O, Fe, Ni and Cr. Table 6 gives the relative amounts detected for selected elements only; the data are representative of nodules both above and below the rolled joint. Also presented in Table 6 is data for a stained area immediately surrounding a nodule. This area also contained a relatively large amount of chlorine.

Table 6. AES Ratios
(see also Appendix 3, Table A7)

Location	$Ni_{/(Ni+Fe+Cr)}$	$Cr_{/(Ni+Fe+Cr)}$	$Fe_{/(Ni+Fe+Cr)}$	$Cl_{/(Ni+Fe+Cr)}$	$O_{/(Ni+Fe+Cr)}$	$C_{/(Ni+Fe+Cr)}$
Nodule	0.54	0.15	0.32	0.52	0.48	2.25
Stain surrounding nodule	0.80	0.00	0.20	0.27	1.37	7.23

Outside the nodular and the surrounding stains the most dominant peaks were for iron, oxygen, and carbon. Small quantities of chlorine and sulphur were also found. Much of the carbon present is from ambient contamination.

5 Discussion

5.1 Metallurgical condition

The metallurgical examinations indicate that the tubing is in generally good condition. The hardness of annealed tubing is expected to be at least 138 H.V.; thus, it would appear that the undeformed tube is of marginally low hardness. This holds no significant implications regarding either mechanical integrity or corrosion performance. Table 1 shows that the tubing conforms to compositional requirements with the exception of a somewhat high sulphur content. Similarly, this should pose no significant problems for tubing performance, although alloy sulphur content can affect corrosion behaviour.

The dual etch revealed an acceptable distribution of carbides along grain boundaries.

5.2 Corrosion damage

There is no gross corrosion damage on the tube. Although there was some evidence of general IGA early in the investigation, other examinations proved that it was not present except in connection with shallow non-uniform corrosion. In this connection, the IGA itself was very shallow and appears to be the precursor of the non-uniform attack and deeper pitting. In its most insidious form, IGA penetrates deeply into the metal with little or no accompanying surface corrosion, although surface grains may drop out when the IGA has surrounded them. This form of IGA is not present on this tube; the observed IGA (of less than $^1/_4$ to $^1/_2$ grain diameter) is better called grain boundary outlining or grooving to distinguish it from deeper IGA.

The presence of a network of intergranular carbides in the tubing microstructure suggests that good stress corrosion cracking performance can be expected. However, if this is accompanied by chromium depletion (i.e. sensitization) then resistance to acid induced IGA may be reduced. Significant IGA does not seem to have developed even though acid sulphate was present, suggesting that the tubing may not be sensitized. This has not been confirmed by specific testing for sensitization.

The presence of non-uniform corrosion and pitting is cause for concern, particularly since it was found throughout the length of the tube, and not confined to the roll transition crevice or a sludge pile.

Extent

The extent of corrosion can be considered to have three main components.

depth	In terms of depth, the observed attack is superficial. At a depth of about 10 µm, the non-uniform corrosion penetrates about 1% of tube wall thickness. The maximum pit depth of 60 µm is only 5% of tube wall thickness.
surface area	In terms of surface area, the attack is slight. Combining the surface dimensions and population suggests that in regions subject to corrosion about 1% of the tube surface area is affected.
degree of distribution	In terms of distribution, the attack is widespread under tube fouling deposits on the tube examined.

The extent of corrosion throughout the entire steam generator is dependent on the degree of tube surface fouling and the formation of locally aggresseive solutions; it cannot be determined from only one tube. However, it is expected that this tube is representative of many in the steam generator; thus, it must be concluded that similar corrosion is present on other tubes.

Causative factors

Several observations provide clues to the possible cause of the observed corrosion.

- The presence of chlorine and sulphur at and in proximity of corrosion sites implicate their involvement in the corrosion process.
- Morphological features of the attack, such as facetting, crystallographic striations, and grain boundary outlining, are consistent with attack by chlorine and sulphur species.

- Examination of a tube from the same boiler, but removed in the spring of 1989 [report M89-59-K], revealed no such corrosion. This strongly implicates the acid excursion of 1989 as the period of corrosion damage.

- The corrosion appears to be associated with the nodular deposits, as indicated in Figure 10.

With this information in mind, the following possible mechanism of corrosion is proposed.

> General tube surface deposits promoted the formation of concentrated chemical environments close to tube surfaces; lake water impurities, particularly chloride ions, can produce solutions that are aggressive towards the tubing. Acid sulphate, introduced during the water treatment plant upset, also contributed to the concentrated environments. Corrosion proceeded under the combined influence of anionic contaminants, particularly chloride and sulphate. Corrosion products then accumulated in the vicinity of active sites, forming nodules and irregularities within the general deposit.

5.3 Deposits

The analytical results show that the deposit above the rolled joint is magnetite with varying amounts of minor constituents. This is consistent with the general crystalline nature of the deposit and with general expectations for boiler tube scales.

The minor constituents included contamination elements normally associated with lake water: Si, Mg, Al, Ca, and Ti. Chlorine was present at relatively high concentrations, and persisted even after lengthy sputtering.

The presence of the charge-shifted Ni shows that it is unlikely to be associated with the bulk phase; rather it is deposited on an insulated oxide or hydroxide substrate. This indicates that conditions have at some time existed which have been conducive to the reduction of nickel compounds. The data also indicates that carbon may be associated with these particles.

X-ray maps for the material contained in the nodules were shown in Figure 14. Clearly, the most predominant elements are iron, chlorine, chromium and nickel. Auger images for Fe, C, Ni, and Cl were given in Figure 16. From these images it is even clearer that the irregularities are rich in chlorine and that there is also nickel associated with them. It is also evident that some parts of the deposit have a high concentration of carbon and little iron.

The data obtained during this examination show clearly that irregularities observed above and below the tube sheet are different from the surrounding material. One of the major components found in these areas was chlorine, an element which is known to adversely effect the integrity of the protective passive film which forms on the surface of this class of material. Relatively large concentrations of this element were observed (10.6 - 11.7 atomic wt %). The source is not known.

In areas below the rolled joint the tube surface is much cleaner. XPS and AES analyses from this area revealed chlorine, chromium, iron, and nickel. The concentration of oxygen on the outer surface was also elevated. EDS detected considerable concentrations of chromium, nickel, and iron largely from the parent tube material. This suggests that other elements found with XPS and AES were present as thin films.

Origins

The general magnetite scale on the tubes is produced by the deposition of carbon steel corrosion products. The bulk of these corrosion products are produced in the feedtrain and transported into the

steam generators as suspended particulate or dissolved species. A major contributor to the production of corrosion products is oxygen introduced by air in-leakage.

These analyses have allowed the characterization of nodules and irregularities on the tube surface. However, their origin is unknown. One possibility is that the nodules are precursors to localized corrosion and a second is that they are the result of localized corrosion, as postulated earlier in the proposed corrosion mechanism.

The contaminants found in both the nodules and the general deposit are normally associated with untreated lake water. It therefore seems probable either that there has been passage of these elements through the ion exchange system, or that lake water has entered the steam generators as a result of condenser leaks.

5.4 Implications

Integrity

Steam generator integrity is not immediately compromised by the degree of attack observed. No more than a 1% strength loss would be expected as a result of the observed corrosion. This should be well accommodated by design margins and safety factors.

Because of the continued presence of tube deposits, aggressive crevice conditions could reform during normal operation or upsets. Continued degradation would pose a threat to tube integrity in the long term.

Other steam generators and reactor units

It is not possible to determine from one tube whether or not other steam generators or units are similarly affected. However, it is reasonable to believe that any tubes with significant deposits are at risk and may have suffered attack.

If the tube examined is considered representative of the unit or the station as a whole, then it must be concluded that this is a generic problem, not a local one. All units of Bruce NGS B have been subjected to similar bulk chemical conditions; therefore, aggressive conditions could have formed in other units as they did in the examined steam generator. Thus, it is expected that steam generators of the other 3 units of Bruce B have suffered attack. This attack may be more or less severe because of the variable amounts of tube deposits on each unit.

Operation

All things considered, the presence of lake water impurities, chronic air ingress, and water treatment plant upsets are believed to be the main contributors to the corrosion. The presence of tube deposits is also importrant since the deposits are sites for the development of locally aggressive conditions. The importance of deposits was noted in the examination of tubes removed from Bruce NGS Unit 1 after an acid excursion there (Bellamy, Gonzalez, and King, 1986). In that case, attack was confined to the area of the tubesheet sludge pile. General tube surfaces, believed to be relatively unencumbered by deposits then, were free of corrosion damage.

The principal implications for operation are that good water chemistry and minimum air inleakage must be rigorously maintained to avoid this sort of corrosion damage. It should be remembered that normal makeup [or even small condenser leaks] can supply sufficient contaminant to generate aggressive conditions. A system to monitor boiler chemistry and to rapidly detect an excursion should be available on all units, and remedial action should be taken immediately in the event of a chemical excursion.

Water chemistry upsets can be better tolerated if tube surfaces are relatively free from deposits. Air ingress is believed to contribute substantially to tube fouling by increasing the quantity of corrosion product entering the boiler as suspended particulate. Also, air ingress will contribute to the transport of dissolved, oxidized species into the boiler, where they can participate in local corrosion reactions.

The presence of attack demonstrates clearly that tube surface deposits are undesirable for long term corrosion performance; significant fouling is cause for concern and all attempts should be made to minimize it. Some appropriate actions to accomplish this are as follows.

- avoid chemical excursions that can contribute non-volatile solutes
- avoid condenser leaks
- minimize oxygen and optimize pH to prevent piping corrosion
- minimize corrosion product transport

6 Recommendations

Although the evidence is mounting, it continues to be difficult to assess the overall extent of corrosion in steam generators. Clearly, though, corrosion does occur. Therefore, the following recommendation are given.

- A system to monitor boiler chemistry and to rapidly detect an excursion should be available on all units.

- Remedial action should be taken immediately in the event of a chemical excursion.

Better information is necessary about the extent of corrosion. For this, a larger sample size is required to represent, adequately, the population of tubes in the bundle and to assign statistical significance to the results.

- It is recommended that additional tubes be obtained for this purpose at every reasonable opportunity.

This would provide baseline information for reference in future condition-monitoring and assessments of steam generator tubes.

7 Conclusions

1. Although the tubing was found to be in generally good condition, the presence of shallow, non-uniform corrosion to a depth of 30 μm and pitting to a depth of 60 μm is cause for concern.

2. Attack was caused by the combined influence of anionic contaminants, particularly chloride and sulphate.

3. The presence of lake water impurities, chronic air ingress, and water treatment plant upsets are believed to be the main contributors to the corrosion.

4. Steam generators of the other 3 units of Bruce B station are likely to have suffered attack. This attack may be more or less severe than that observed in unit 6.

5. Analyses indicate that the deposits contain mainly iron, with varying amounts of nickel and chromium, and trace amounts of titanium, calcium, and silicon. Chlorine and sulphur were identified in several analyses, particularly in connection with nodular deposits and other irregularities.

6. Tube surface deposits pose a substantial threat to tubing integrity.

Acknowledgements

The facilities and staff of Surface Science Western have contributed to the information presented here, particularly for deposit analyses. Sample preparation, metallography, and scanning electron microscopy were capably performed by Bonnie Guest, Dave Limoges, and Fred Smith. Dr. F. Gonzalez of the Corrosion Chemistry Section, Chemical Research Department, provided useful assistance in the interpretation of deposit chemistry data.

Recommended by:

P.C. Lichtenberger
Supervisng Scientist
Corrosion and Tritium Technology Section
Metallurgical Research Department

Approved by:

J. Brown
Manager
Metallurgical Research Department

Submitted by:

Peter J. King
Corrosion Engineer
Corrosion and Tritium Technology Section
Metallurgical Research Department

Alexander M. Brennenstühl
Corrosion Engineer
Corrosion and Tritium Technology Section
Metallurgical Research Department

Graham Bellamy
Senior Engineer
Metallurgy Section
Metallurgical Research Department

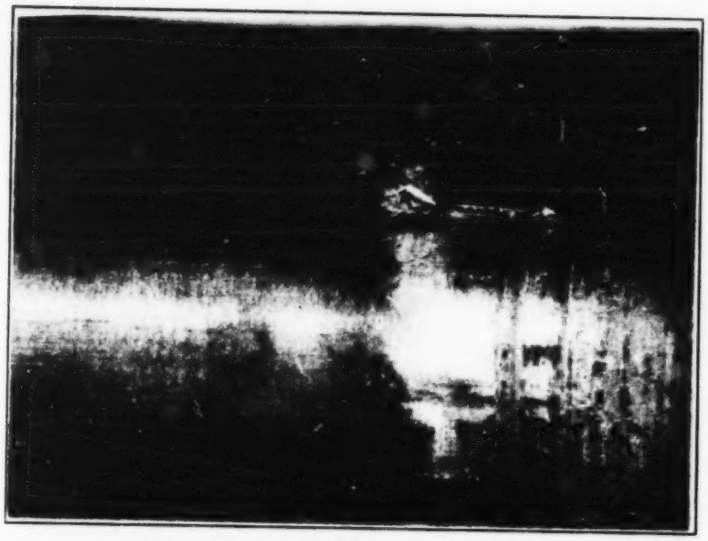

a) Optical micrograph showing the region below the rolled joint. A circular discoloured region can be seen just to the left of and below the centre of the photograph. The rolled joint itself is to the right of the photograph.

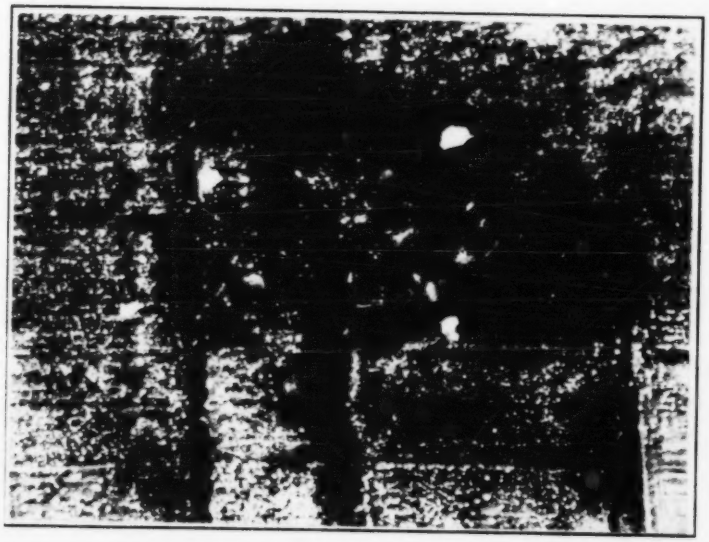

b) Scanning electron micrograph of a nodule and the general surface deposit above the rolled joint. The scratches seen here are pre-existing from surface grinding and fabrication; they are not the result of tube removal.

Figure 1 Illustrations of the general surface features of tube R57S32.

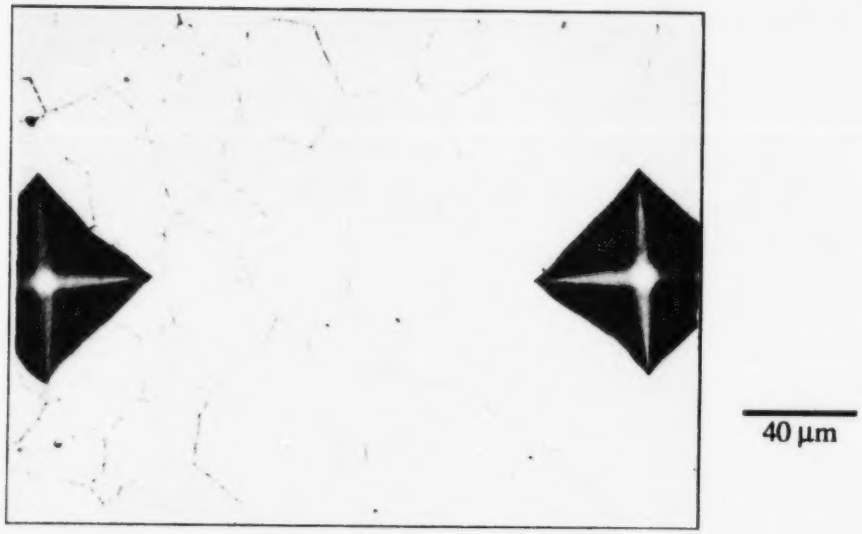

a) Micrograph showing the carbide structure as revealed by an electrolytic orthophosphoric acid etch.

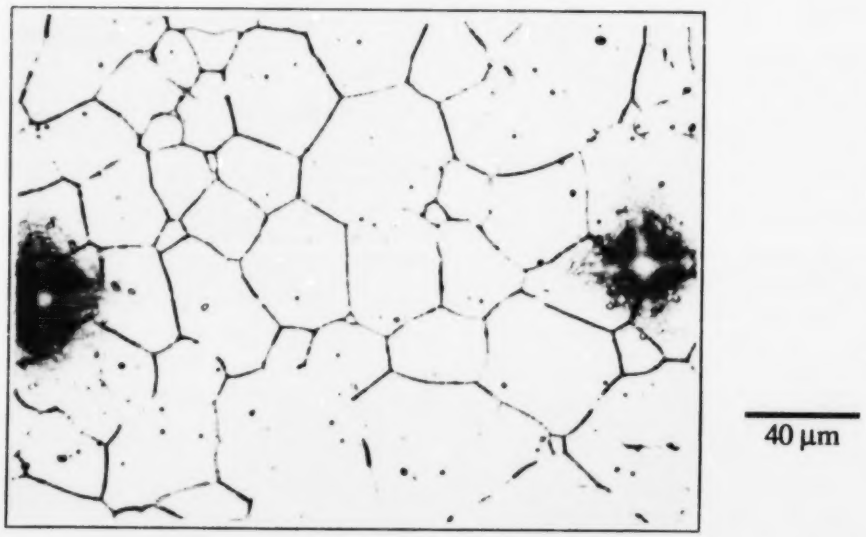

b) Micrograph showing the grain boundary structure as revealed by an electrolytic nital etch.

Figure 2 The general microstructure of tube R57S32. Comparison of a) and b) reveals that a nearly continuous distribution of carbides exists at the grain boundaries. This structure is considered to be resistant to intergranular stress corrosion cracking.

a) Tube surface below the rolled joint.

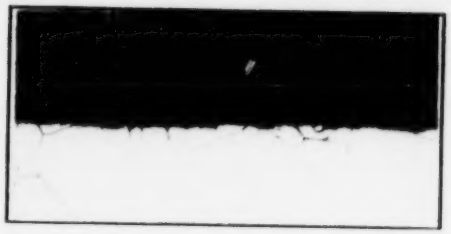

b) Tube surface above the rolled joint. The thick deposit is clearly visible.

Figure 3 Cross-sections of the tube at the outside surface showing general microstructural features. The possibility of shallow intergranular attack is suggested by enhanced etching of grain boundaries at the tube surface. This was not borne out by subsequent examinations.

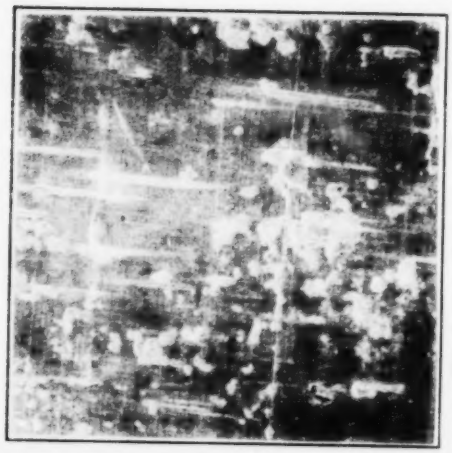

a) Low magnification micrograph showing scattered areas of shallow non-uniform corrosion and unattacked metal surface in between.

b) Same area as a) at a higher magnification showing details of the corrosion. Crystallographic striations and grain boundary highlighting are apparent at the top of the picture.

Figure 4 Micrographs of tube R57S32 after chemical descaling by APAC, showing the outside surface of the tube above the rolled joint. Note the nature of the corrosion and the absence of general intergranular attack. See also Figure 5.

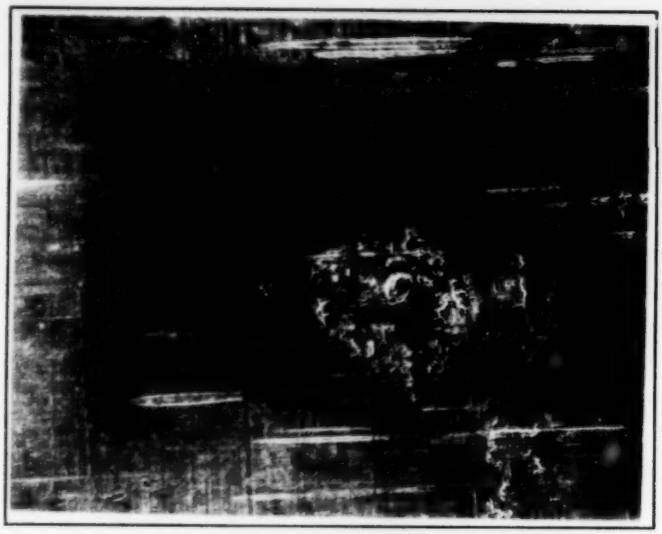

a) Low magnification micrograph showing a pit wihin an area of shallow corrosion in the centre of the picture. Other areas of shallow attack can be seen to the right of and below the central site.

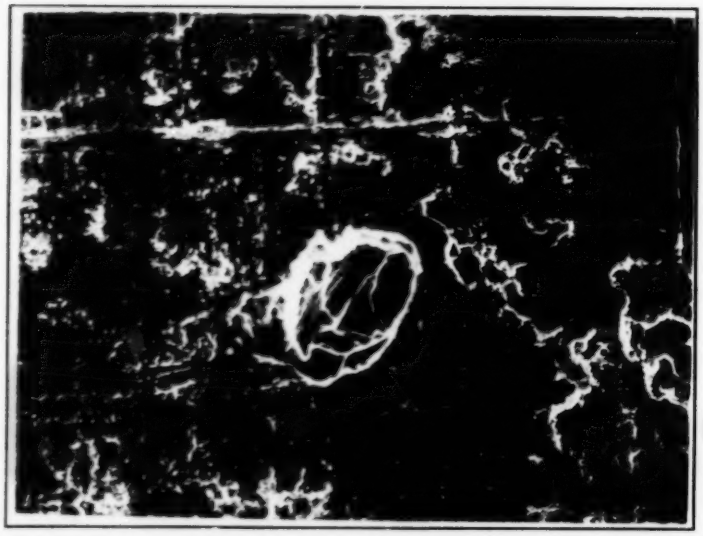

b) Higher magnification micrograph of the central site in a) showing detatils of the attack morphology. Note facetting and striations within the pit. The pit is about 40 µm in diameter and about 20 µm deep.

Figure 5 Micrographs of tube R57S32 after chemical descaling by APAC, showing corrosion on the outside surface of the tube above the rolled joint. See also Figure 4.

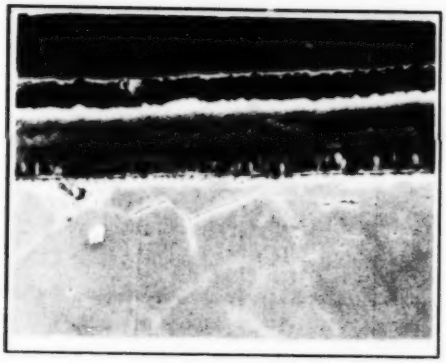

a) A view showing the general multi-layer structure of the thick deposit. The deposit appears to be dense and of low porosity, with a smooth topography.

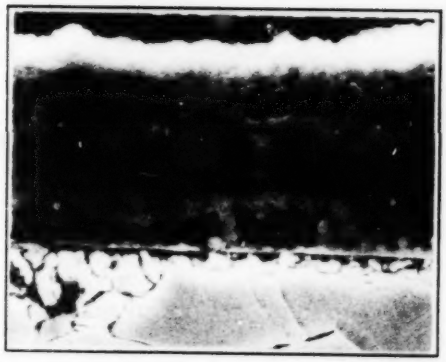

b) The region at the top of a) at a higher magnification showing further detail of the layers. Note the very thin oxide film at the metal surface and the granular appearance of the metal beneath, indicating a possible corrosion site.

Figure 6 Scanning electron micrographs of a cross-section through the deposit layer above the rolled joint on tube R57S32.

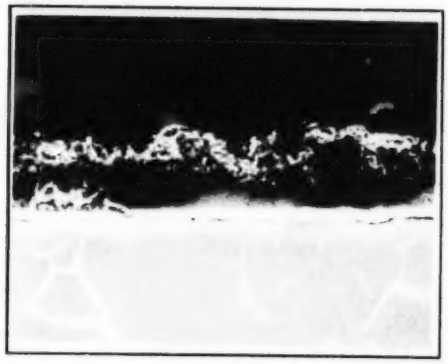

a) A view showing the general structure of the deposit. The deposit appears to be of higher porosity than that shown in Figure 6. Note also the very rough topography.

b) The region near the centre of a) at a higher magnification showing further detail of the deposit. A very thin oxide film is apparent at the metal surface as shown in Figure 6; however, in this case there is no indication of corroison beneath it.

Figure 7 Scanning electron micrographs of a cross-section through the deposit layer above the rolled joint on the tube removed in early 1989, prior to the water treatment plant excursion.

a) A micrograph showing deposit from above the rolled joint. A nodule displaying micro-cracking can be seen in the lower centre of the picture.

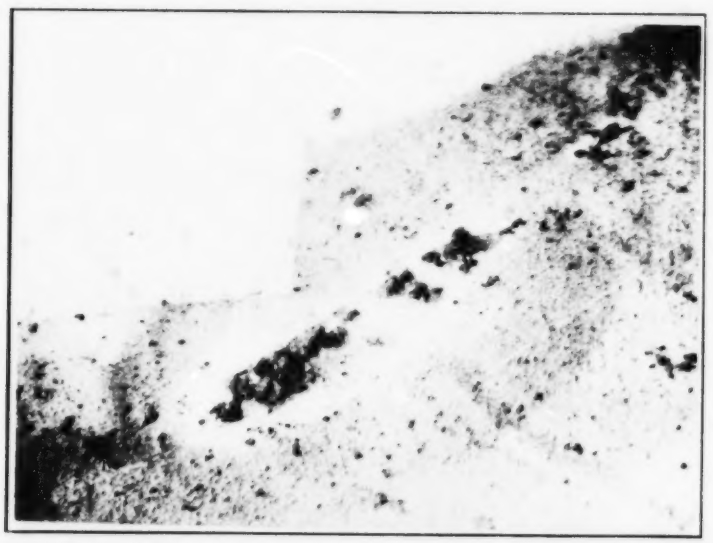

b) A micrograph showing deposit from below the rolled joint. A large nodule can be seen in the centre of the picture.

Figure 8 Outside surface condition of tube R57S32.

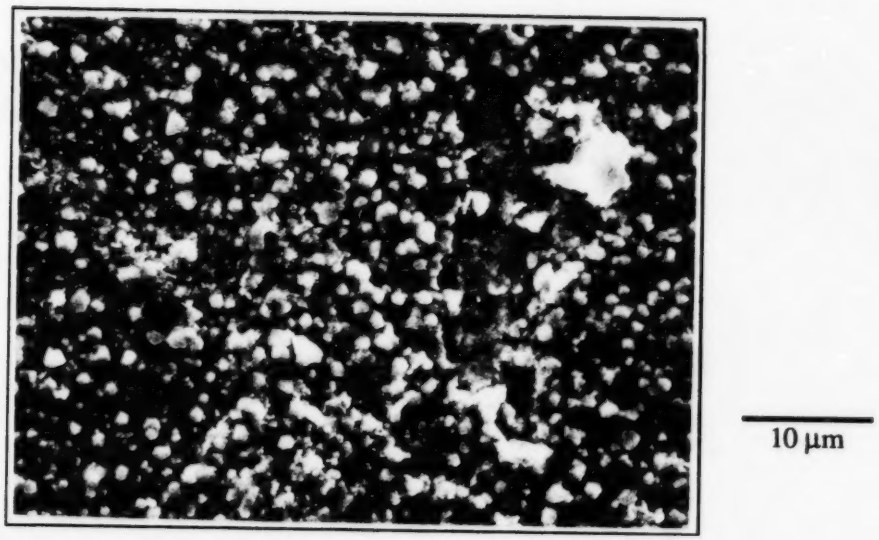

Figure 9 **Another micrograph of the outside surface of tube R57S32 showing the crystalline nature of the deposit.**

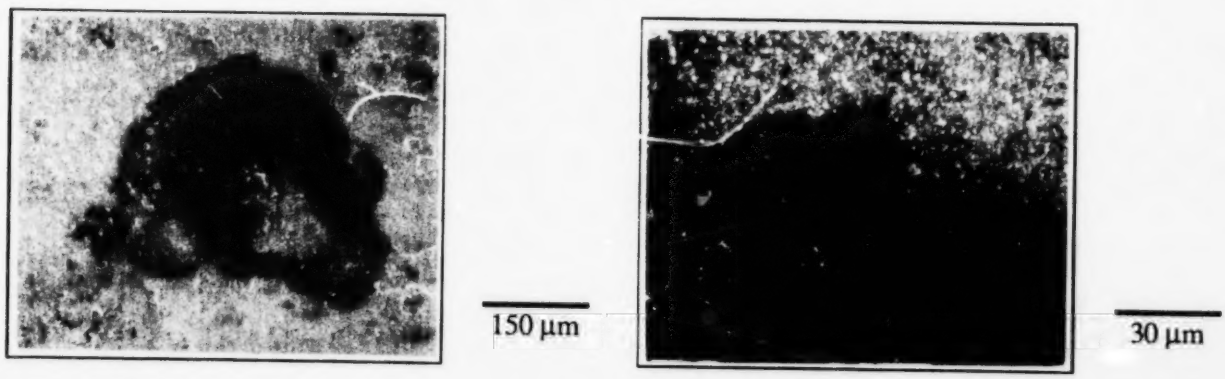

a) A view at low magnification showing the circular nature of the discoloured area.

b) A view at higher magnification showing the similarity in appearance of the two regions. Compositional differences result in the contrast between the areas.

Figure 10 **A micrograph of the outside surface of tube R57S32 showing an area of discolouration above the rolled joint.**

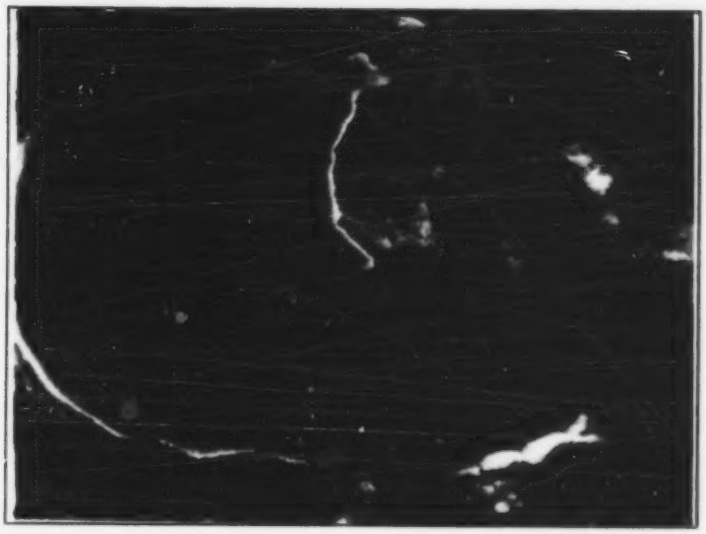

Figure 11 A nodule above the rolled joint showing outer and inner micro-cracked layers, and a small area of oxide covered metal to the right of centre.

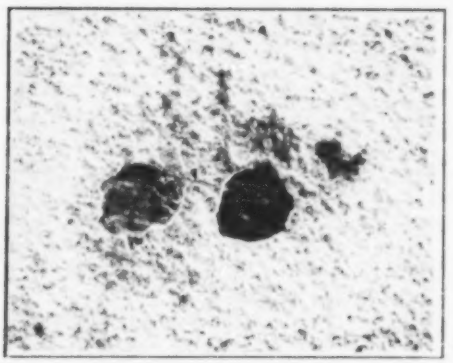

a) A general view showing two spalled patches. The dark area surrounding these suggests that they are part of the same nodule.

b) A higher magnification view of the inner layers of a nodule. Some amorphous deposits and oxide covered metal are visible.

Figure 12 General features within a nodule after removal of the outer layer.

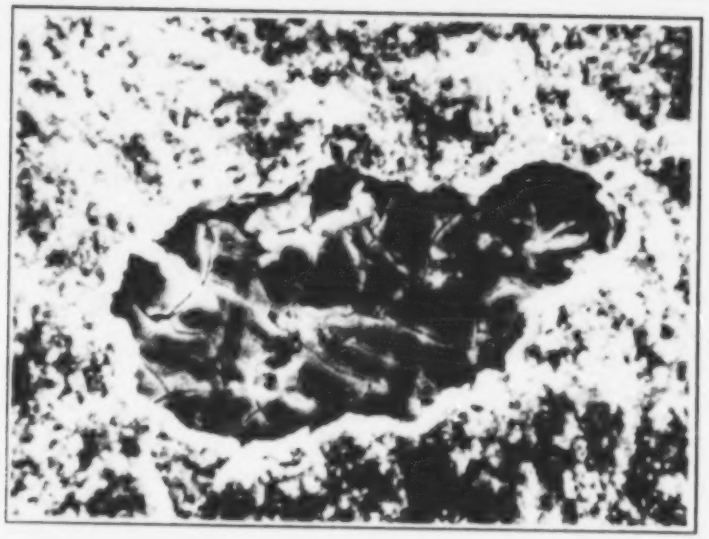

a) The amorphous, micro-cracked inner layer is clearly visible in this photograph.

b) This view shows an area of oxide covered metal.

Figure 13 Details of features within a nodule after removal of the outer layer.

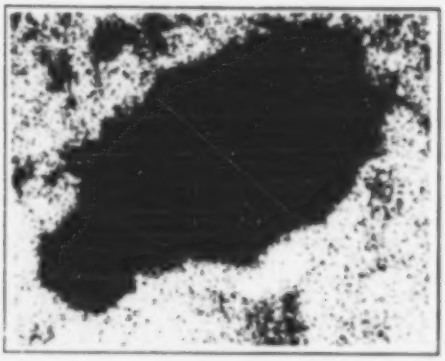

a) Fe map. Note the general absence of iron within the nodule.

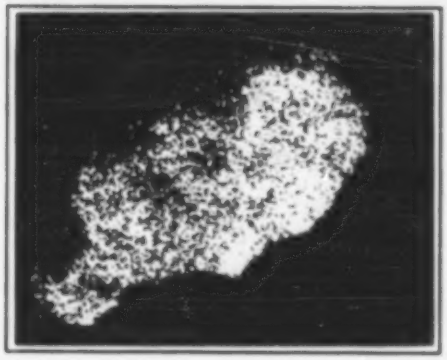

b) Ni map. Nickel is evenly distributed inside the nodule.

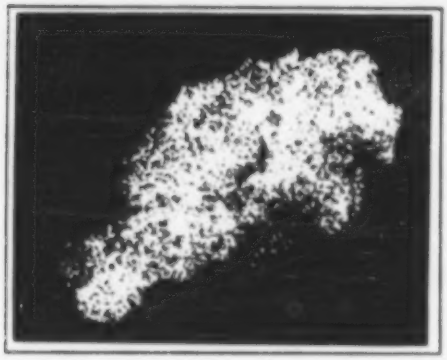

c) Cr map. Although well distributed, there are some regions in the nodule that are low in chromium.

d) Cl map. Chlorine is unevenly distributed inside the nodule. Close examination reveals that high Cl corresponds with high Ni and low Cr.

20 µm
(all images)

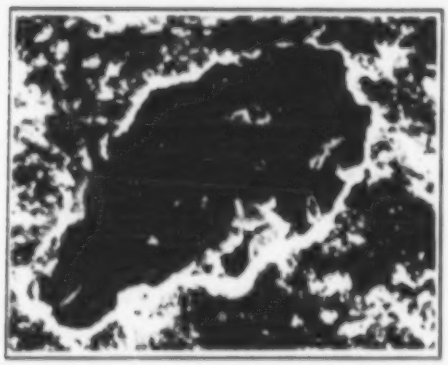

e) Secondary electron image of nodule.

Figure 14 EDS maps for the nodule shown in Figure 13a.

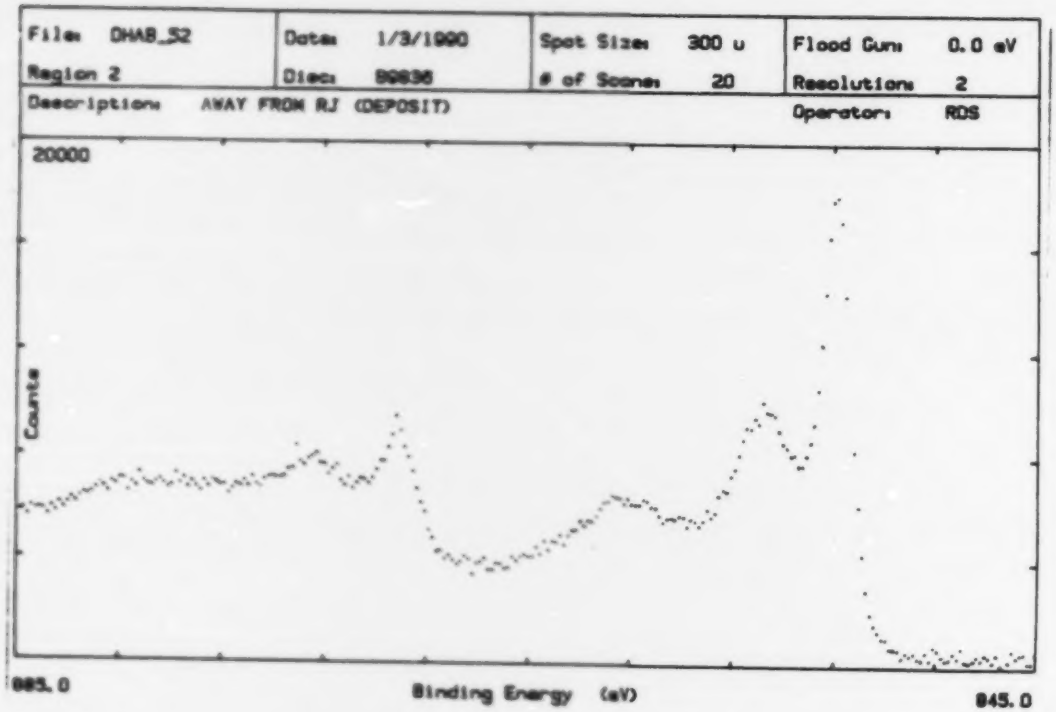

Figure 15 A portion of the XPS spectrum for the general deposit above the rolled joint showing the nickel peaks. The two main peaks are for $Ni(OH)_2$ and Ni metal.

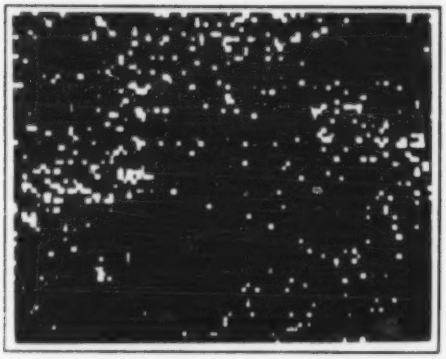

a) Fe map. Note the general absence of iron within the nodule.

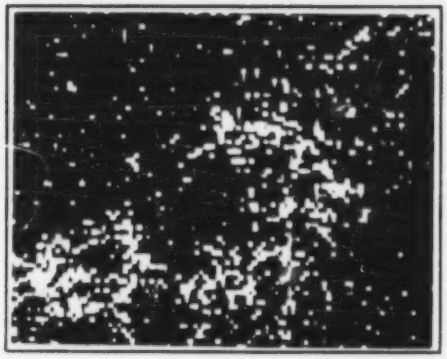

b) Ni map. Nickel is evenly distributed inside the nodule.

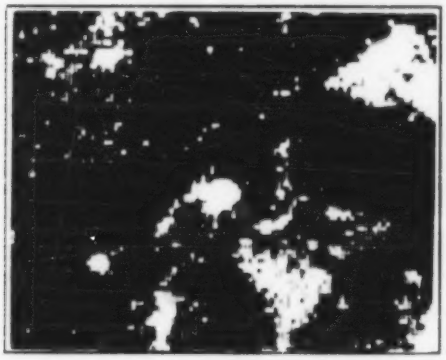

c) C map. Carbon is unevenly distributed and appears particularly where Fe is low.

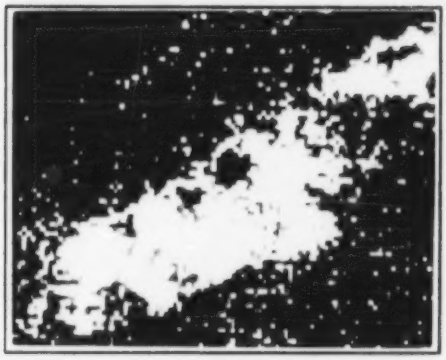

d) Cl map. Chlorine is evenly distributed inside this nodule. Again, high Cl corresponds with high Ni.

150 μm
(all images)

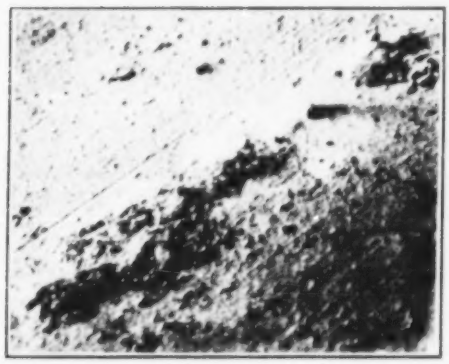

e) Secondary electron image of nodule.

Figure 16 AES maps for the nodule shown in Figure 8b after 1 minute of sputtering.

APPENDIX 1

POLISHING AND DUAL ETCH PROCEDURE FOR N06600

GENERAL

The following instructions are supplementary to standard metallographic practices of specimen preparation and examination.

SECTIONING

The sample shall be cross-sectioned at identified locations using a fretsaw or miniature hacksaw. Care should be taken in clamping and cutting to avoid affecting the structure of the metal, with the following specific aims.

- to produce a flat surface
- to minimize mechanical (plastic) damage
- to minimize burr formation on, or other damage to, the edge to be examined

Cut sample pieces should be appropriately identified so that the origin and orientation of each can be traced.

Grinding of the face to be examined, to remove burrs or to flatten, is permitted prior to mounting, provided that the edge to be examined does not become rounded and that a minimum of material is removed (i.e. the finished face is not moved far from the desired section location).

MOUNTING

Each specimen should be cleaned, de-greased, and mounted either in a thermosetting, filled, dry epoxy resin, or in a castable epoxy resin. Epoxy resins are chosen to provide good sample adhesion, low shrinkage, and good hardness, all of which contribute to good edge retention. It is recommended that the sample identification be scribed on the side or back face of the mount.

POLISHING

The mounted samples should be ground on a series of metallographic papers of increasing fineness. Final polishing is to be carried out on a microcloth using a 0.3 μm or better paste or abrasive suspension.

Considerable care should be exercised to minimize rounding of the edge to be examined.

MARKING

The polished surface is to be marked with three microhardness indentations in an arrangement that allows unambiguous orientation of the sample when performing metallographic examination and obtaining photomicrographs. The indentations should be close to a crack if possible and remote from an area that will be used to make electrical contact during electrolytic etching.

A weight of 50 g [force] produces a mark of about 50μm, and is suitable in most cases.

ETCHING

EQUIPMENT AND SET-UP

The required etching voltage is to be supplied by a constant voltage DC power source. A potentiostat or a laboratory power supply (such as HP model 6214C) are suitable for this purpose. It may be necessary to use a voltage divider with the potentiostat if its reference adjustment does not allow a setting of three volts. The output voltage should be checked with a digital voltmeter to ensure correct polarity and voltage setting within the prescribed limits. The sample to be etched should be made the anode and a platinum wire should be used as the cathode. Contact with the sample should be made with a pointed platinum probe. Stainless steel or alloy 600 can be used as an alternative to platinum, but are less desirable.

The following figure illustrates possible set-up configurations. The values of resistance in the voltage divider are not critical. They should be chosen to permit easy adjustment to three volts (counter to working), but should be large enough not to cause undue load on the potentiostat.

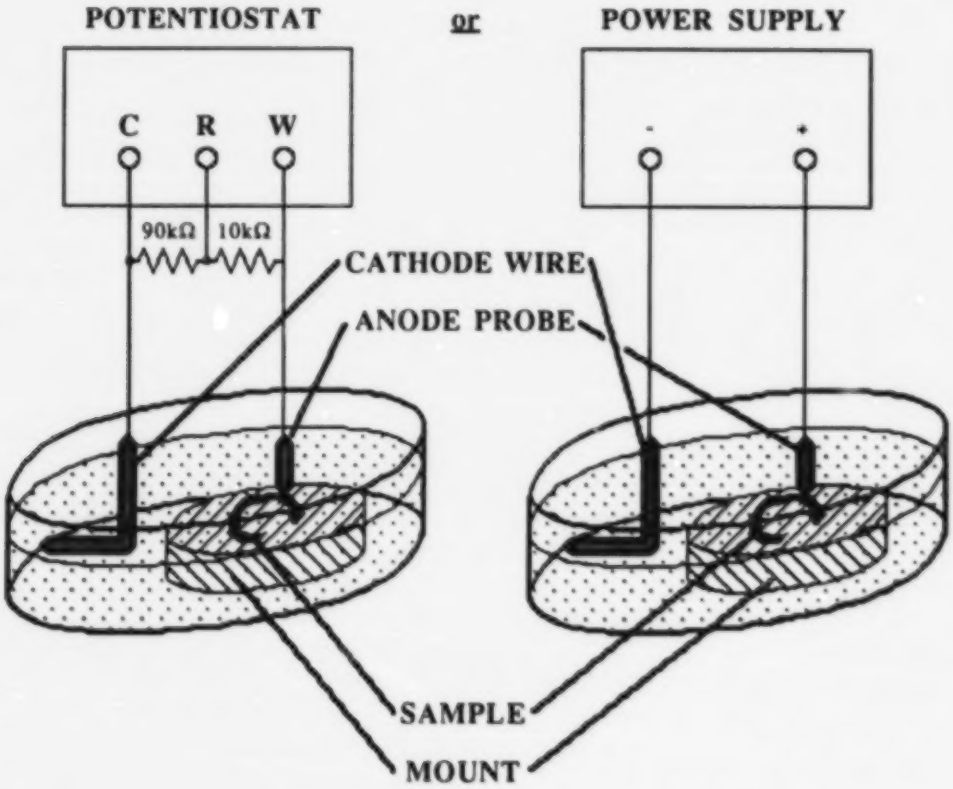

GENERAL ETCHING PROCEDURE

The etchants should be contained in shallow glass dishes of such dimensions that the entire mounted sample can be submerged.

The following steps should be taken.

1] Turn on the power supply.

2] Place the sample to be etched in the solution.

3] Make electrical contact to the sample with the anode probe. Exercise care to make a firm contact away from the marked area and avoid scratching the polished surface.

4] Start etching by immersing the cathode wire while maintaining anode contact.

5] Stop etching after the prescribed time has elapsed by removing the cathode wire from the solution.

6] Carefully remove the anode probe to avoid scratching the polished surface.

7] Remove the sample from the etchant, rinse with deionized water, rinse with alcohol, and dry.

8] Examine under the microscope.

9] Repeat steps 2] through 8] as required

The orthophosphoric acid etch should be performed first, followed by the nital etch. ***Do not polish between etches.*** Photomicrographs obtained at each stage should be of the same area so that carbide and grain boundary structures can be compared directly.

ORTHOPHOSPHORIC ACID [ELECTROLYTIC]

Etching Solution	10 mL Deionized water 80 mL Orthophosphoric acid
Etching Voltage	3.00 ±0.01 Volts

Etch for up to 40 seconds. Normally less than 20 seconds is sufficient to produce a fully developed carbide structure.

If the sample is over-etched it should be re-polished to remove all visual traces of the etch and then re-etched for a shorter time.

Over-etching can result in additional features appearing [slip lines, twin boundaries, etc] and in loss of definition of the carbide structure itself. Therefore, an initial trial is suggested when etching an unknown structure. Successive 5 second etches, with microscopic examination after each, will determine the optimum etching time. Subsequent etching can then proceed with a single, fixed-time exposure. The optimum etching time is that after which no further carbide structure appears and before image degradation. A series of photomicrographs, one after each 5 second trial etch can assist in making comparisons.

Once a suitably etched surface has been produced, photomicrographs should be obtained at magnifications of x200 and x400. The microhardness marks should be positioned to one side of the image field.

NITAL [ELECTROLYTIC]

Etching Solution **DO NOT STORE** (prepare fresh daily)	95 mL Methanol (absolute) 5 mL Nitric acid (70%)
Etching Voltage	3.00 ±0.01 Volts

Etch for up to 40 seconds. Normally less than 20 seconds is sufficient to reveal grain boundaries.

Over-etching should be carefully avoided, since re-polishing also requires a repeat of the orthophosphoric acid etch.

Over-etching can result in additional features appearing [slip lines, twin boundaries, etc] and in overall image degradation. Therefore, an initial trial on a polished [not orthophosphoric etched] sample is suggested when etching an unknown sample. Successive 5 second etches, with microscopic examination after each, will determine the optimum etching time. Subsequent etching can then proceed with a single, fixed-time exposure. The optimum etching time is that after which no further grain boundaries appear and before image degradation occurs. A series of photomicrographs, one after each 5 second trial etch can assist in making comparisons.

Once a suitably etched surface has been produced, photomicrographs should be obtained at magnifications of x200 and x400. The microhardness marks should be positioned to one side of the image field and the same area should be included as was viewed after the orthophosphoric acid etch.

APPENDIX 2

APAC DESCALING PROCEDURE

The following procedure is used to removing magnetite scales from the surface of nickel alloys N06600 and N08800.

Normal chemical handling and safety procedures should be followed; wear eye and face protection.

Step 1

Solution	30 g/L $KMNO_4$ 100 g/L NaOH
Exposure	Immersion for 45 minutes at solution boiling point under a nitrogen blanket.

Rinse between steps

Loose scale can be removed by gentle brushing or rubbing with a pink eraser. If the surface is sufficiently descaled, step 2 can be omitted.

Step 2

Solution	100 g/L $(NH_4)_2$citrate 3 ml/L OSI-1 inhibitor
Exposure	Immersion for 1 hour with solution at 90 °C to 95 °C under a nitrogen blanket.

APPENDIX 3

Table A1 Semi-quantitative EDS

Location	Element (Wt.% conc)											
	Fe	Cr	Ni	Ca	Mn	Si	Mg	Al	K	Ti	Cl	S
Black deposit, above rolled joint	76	3	8	3	2	3	0	1	1	1	0	2
Nodular, micro-cracked deposit, below rolled joint	13	34	28	2	7	1	1	0	0	4	6	4

Legend for Table A2
(following page)

Codes	Comments
1, 2	BR335 mounted cross section containing rolled joint
4, 5, 6, 7, 10, 12, 13	BR335 unmounted section containing rolled joint
14, 15	BR335 unmounted section containing rolled joint, APAC cleaned
16, 17, 18	BR313 mounted cross section containing rolled joint
BR313	tube removed spring 1989
BR335	tube removed November 1989
M	major
md	medium
m	minor
tr	trace
x	not detected
bkgd	approximate background counts level

Table A2 Qualitative EDS

Code	Location		Element (relative amount or peak height)					
			Fe	Ni	Cr	Cl	Ti	Others
1a	just above roll transition	inner scale	M	m	tr	tr	x	Ca, Si
1b		outer scale	M	tr	x	x	x	—
2a	nodule just above roll transition, 180° from 1	inner scale	M	m	tr	x	tr	Al, Ca, Si, Mg
2b		outer scale	M	m	x	x	tr	Mg
2c		inner nodule	M	tr	tr	x	x	—
2d		oxide film [?]	1105	685	421	x	x	—
2e		metal	403	1674	662	x	x	—
4a	about 5 mm from roll transition	general deposit	M	m	x	x	x	—
4b		dark spot	M	m	tr	tr	tr	—
4c		adjacent to spot	M	m	tr	x	tr	—
5	within 1 mm of roll transition	dark spot 1	M	md	m	tr	x	—
6		dark spot 2	M	md	m	x	x	—
7		adjacent area	M	m	m	x	x	—
10a	about 20 mm from roll transition	deposit on exposed metal	276	1261	787	430	x	—
10b		exposed metal	447	2459	963	157	x	—
12	about 15 mm from roll transition	exposed metal	1071	3567	1595	x	x	—
13a	about 10 mm from roll transition	dark spot	1974	189	129	x	x	bkgd about 100 - 120
13b		centre light area	1988	911	576	x	x	bkgd 120
14	within 1 mm of roll transition	corroded area	209	792	300	x	x	bkgd 73
15		base metal	226	958	343	x	x	bkgd 80
16a	within 2 mm of roll transition	metal	445	2175	971	x	x	Mn bkgd 70 - 80
16b		scale	2114	235	73	x	98	Mn bkgd 30 - 40
17	within 1 mm of roll transition	scale	2085	117	72	X	80	Mn 87 bkgd 25 - 45
18a	within 1 mm of roll transition, 180° from 17	scale	2049	108	61	x	94	Mn 98 bkgd 40 - 60
18b		scale, spot analysis 2 µm from metal	2095	264	79	x	100	Mn 69 bkgd 30 - 60
18c		metal, spot analysis near surface	630	2113	882	x	105	Mn 146 bkgd 60 - 80

Table A3. XPS summary

Location	Element (Atomic %)									
	O	C	Cl	Si	Ni	Fe	P	Cu	Cr	Ca
Tarnish film, below rolled joint [sputter time 300 secs.]	30	38.8	0.9	-	5.7	19.2	-	-	2	0.3
nodule, below rolled joint [sputter time 300 secs.]	38.1	20.1	0.7	2	5.6	28.4	-	-	1.1	0.8
deposit, above rolled joint [sputter time 60 secs.]	24.4	60.2	1	2.6	0.5	5.3	1.1	0.5	0.2	0.6

Table A4. XPS composition from the bronze film on the tube surface below the rolled joint

Sputter Time	Element (Atomic %)														
(sec)	O	Na	Ti	N	Mg	C	Ar	Cl	Si	Al	Ni	Fe	Mn	Cr	Ca
0	14	0	-	2.7	-	78.7	-	0.9	0.4	-	1.6	0.5	-	-	-
30	13.1	0.7	-	2.7	-	74.2	-	1.1	0.5	1	2.9	3.1	-	-	0.5
160	20.9	0.2	0.2	2.4	-	55.5	-	0.9	2.3	1.9	4.9	9.9	-	0.3	0.6
300	30	0.6	0.2	0.9	-	38.8	-	0.9	-	1.6	5.7	19.2	-	2	0.3
600	37.6	0.5	0.2	1.8	0.7	21	-	0.4	0.3	4.2	6.9	20.4	0.8	5.5	-

Table A5. XPS composition from a nodule below the rolled joint

Sputter Time	Element (Atomic %)														
(sec)	O	Na	N	Ca	Mg	C	Cl	Ar	S	P	Si	Al	Fe	Cr	Ni
0	22.1	0.9	2.3	1.3	0.7	53.5	1.8	-	0.3	0.3	1.5	1.8	7.1	0.3	6
30	29.6	0.6	2.5	1.3	0.5	37.7	2.1	-	-	-	1.1	1.9	15.6	0.6	6.4
120	32.1	0.3	1.3	1.4	0.8	30.7	1.4	-	-	-	2.4	1.2	21.1	1.1	6
300	38.1	-	1.2	0.8	0.5	20.1	0.7	-	-	-	2	1.6	28.4	1.1	5.6

Table A6. XPS composition from the deposit above the tube sheet

Sputter Time	Element (Atomic %)														
(sec)	Cu	Fe	O	Na	N	Ca	Mg	C	Cl	P	Si	Ni	Cr	Ti	K
0	0.1	0.3	18.9	0.8	0.9	0.4	1	75.1	0.3	0.4	1.7	-	-	-	-
60	0.5	5.3	24.4	1.4	0.9	0.6	1.1	60.2	1	1.1	2.6	0.5	0.2	0.1	0.2

Table A7. AES Spectra from the Irregularities (Atomic %)

Location	Element									
	Cl	C	N	Ca	O	Fe	Ni	Cr	Si	S
Deposit	10.6 (11.7)	57.3 (50.6)	5.0 (1.7)	1.0 (2.9)	10.3 (10.7)	4.9 (7.1)	8.5 (12.1)	2.3 (3.3)	--	--
Stain Around Deposit	2.6	68.7	3.9	0.9	13	1.9	7.6	-	0.6	0.8

Note: Data in parentheses was obtained after sputtering for one minute with 4 keV argon